Bioactive Poly(ethylene terephthalate) Fibers and Fabrics: Grafting, Chemical Characterization, and Biological Assessment

G. Pavon-Djavid,[†] L. J. Gamble,[‡] M. Ciobanu,[†] V. Gueguen,[†] D. G. Castner,[‡] and V. Migonney*,[†]

Laboratoire de Biomatériaux et Polymères de Spécialité (LBPS/B2OA−UMR 7052) Institut Galilée, Université Paris 13, 99 Avenue Jean-Baptiste Clément, 93430 Villetaneuse, France, and National Electron Spectroscopy for Chemical Analysis and Surface Analysis Center for Biomedical Problems, Departments of Bioengineering and Chemical Engineering, Box 351750, University of Washington, Seattle, Washington 98195-1750

Received March 27, 2007; Revised Manuscript Received August 20, 2007

The grafting of poly(sodium styrene sulfonate) (pNaSS) onto ozone-treated poly(ethylene terephthalate) (PET) fabric surfaces was characterized by X-ray photoelectron spectroscopy and toluidine blue colorimetry. Significant amounts of pNaSS were grafted over the range of experimental conditions examined in this study (30−120 min of ozonation, reaction at 65 or 70 °C, and reaction times up to 240 min). Within these ranges the amount of grafted pNaSS increased with both ozonation time and reaction temperature. The amount of grafted pNaSS increased over the first 60 min of reaction, then remained relatively constant from 60 to 240 min. For the biological experiments pNaSS-grafted samples were prepared with 30 min of ozonation and 60 min of reaction at a grafting temperature of 70 °C. The ozonation time was limited to 30 min to minimize any possible degradation of the PET fabrics by the ozonation treatment. The pNaSS-grafted PET surface adsorbed a factor of 4 more compared to the nongrafted surfaces. The strength of fibroblast adhesion was an order of magnitude higher on pNaSS-grafted PET fabrics compared to that on nongrafted PET fabrics. This difference in the cell attachment was correlated to the cell spreading, which was better and more homogeneous on the grafted fibers compared to the nongrafted fibers. Fibroblasts adhered more strongly on surfaces precoated with normal human plasma compared to surfaces precoated with 10% fetal calf serum in Dulbecco's modified Eagle's medium.

1. Introduction

Poly(ethylene terephthalate) (PET) has been widely used in several biomedical applications, especially when the mechanical properties required fibers and fabrics.[1−4] As a matter of fact, for many years PET was the only synthetic material used for fabrication of vascular grafts.[5] Today it remains a major polymer for vascular graft applications.[6] Many efforts have been made to improve PET's "biocompatibility" and/or "hemocompatibility" with limited success. Thus, improving the biocompatibility of PET remains a topic of investigation.[7,8]

In the 1980s many polymers such as PET, poly(propylene), poly(amide), poly(tetrafluoroethylene) along with carbon fibers were tried as materials for preparing fabrics and fibers for the fabrication of synthetic ligaments.[9] The lack of quality control, poor polymer characteristics (quality, purity, and grade), as well as the absence of controlled washing and conditioning of fibers and fabrics after the processing led to systematic and dramatic failures—mainly originating from fabric abrasion, ligament tears, and weak integration—and severe chronic inflammation in the operated knee joint.[10]

Because of the failures experienced using synthetic ligaments, the orthopedics community stopped using them and went back to the classical method of ligament reconstruction with autogenic tendon grafts. While the success of this technique is high and its use widely recommended in more than 90% of the cases, the time required to recover from this surgery and regain normal physical performance remains too long.[11] Today investigations to improve synthetic ligaments for biomedical applications include advanced polymer science, new surgical techniques, and development of original techniques for weaving and knitting PET fibers and fabrics.[12−15]

As a better understanding of the host-response mechanism has developed, the scientific community interested in synthetic ligaments has focused on the importance of the quality and control of polymer properties for use in a new generation of synthetic ligaments. The recent results of synthetic ligament implantation are positive with regard to good surgical techniques.[12,14−16] However, such surgeries are limited to the small percent of patients that really need a rapid anterior cruciate ligament (ACL) repair (e.g., professional athletes).

In addition, the advancements of specific surface treatments to improve the "host response" and "biocompatibility" of polymers and metallic surfaces led us to develop a method of PET surface grafting for production of a new synthetic biointegrable ACL.[13,17]

The biological causes of synthetic ACL rupture are still the main reason for failure of these devices.[18,19] It should be possible to overcome this issue by developing synthetic ligaments with bioactive surfaces that mask the synthetic origin of the PET prosthesis and allow it to fully integrate with the body. Indeed, weak tissue integration, which leads to ACL rupture and failure, is closely related to the negative host response toward PET.[10] In most failures, the pathologic response was related to the formation of immature collagen on the prosthesis surface, which

* Author to whom correspondence should be addressed. Phone: +33(0)149403352. Fax: +33 (0)149402036. E-mail: vmig@galilee.univ-paris13.fr.

[†] Université Paris 13.

[‡] University of Washington.

10.1021/bm070344i CCC: $37.00
Published on Web 10/11/2007

leads to uncontrolled fibroblast cell response and the accumulation of unstructured fibrous tissue.[10] The host response of PET must be improved to achieve full biointegration of the synthetic ACL. One possible method for improving the host response is to graft bioactive polymers onto the surface of the synthetic ACL.

The grafting of poly(sodium styrene sulfonate) (pNaSS) was first studied on PET films, and those results have been published.[13] In this study pNaSS grafting is applied to PET fabrics, fibers, and total ligaments. The fibroblast cell response to the grafted materials was studied along with protein adsorption from single-component protein solutions, mixed protein solutions, and blood plasma to examine the biological activity of pNaSS-grafted PET surfaces. The surface chemistry of this "new material" was characterized by X-ray photoelectron spectroscopy (XPS) and toluidine blue (TB) colorimetry. The pNaSS-grafted materials were found to preferentially adsorb adhesive proteins and to control fibroblast proliferation, similar to the behavior of natural ligaments. Moreover, it was observed that the presence of proteins deposited from plasma onto the grafted surfaces enhanced the adhesion strength of cells on those surfaces.

2. Materials and Methods

2.1. PET Sample Preparation. Previously we described the results from pNaSS grafting experiments on PET films.[13] The results from that study were used to determine the experimental conditions for grafting pNaSS to PET fabrics in the present study.

The knitted fabrics were provided by the LARS Company (Arc sur Tille, France) and were fabricated by the same process used to produce artificial ligaments. The samples used for the grafting procedures were knitted PET fabrics that were 1×1.3 cm^2 in size and 1.04 mm in thickness. PET fabrics were washed sequentially at ambient temperature, first for 15 min in tetrahydrofuran (THF), then for 15 min in double-distilled water, and finally for 15 min in a boiling aqueous solution of 5% Na_2CO_3. The samples were then dried under vacuum at 65 °C for 30 min.

Ozonation treatment was carried out in an ozone generator (Ozonair). Optimal ozonation conditions were found to be the following: room temperature, 0.6 L/min oxygen, and 100 V. Under these conditions it was assumed that the ozone concentration in aqueous solution can reach 3% (v/v). Six PET fabrics samples were placed in 70 mL of double-distilled water and exposed to the ozone flow for 30, 60, or 120 min. Immediately after ozonation, each piece of PET fabric was put into 3 mL of a NaSS aqueous solution (15% g/v), under stirring and argon atmosphere. Grafting temperatures studied were 65 and 70 °C. Polymerization kinetics was measured over 3 h. After grafting the sample was removed and extensively washed with double-distilled water for 1 h.

Prior to the cell adhesion and proliferation experiments, PET fabrics were extensively washed with 1.5 and 0.15 M aqueous sodium chloride solutions and water then sterilized by UV light exposition for 15 min on each side. Prior to the cell seeding, fabrics were (a) equilibrated at physiological pH with phosphate-buffered saline (PBS), (b) introduced into the wells of a commercial 24-well microtest plate (Costar), (c) incubated overnight in Dulbecco's modified Eagle's medium (DMEM, Invitrogen), and then (d) incubated in 10% fetal calf serum (FCS)-supplemented DMEM.

2.2. Grafting Characterization. *2.2.1. X-ray Photoelectron Spectroscopy.* All XPS data were acquired with a Surface Science Instruments S-probe spectrometer. This instrument has a monochromatized Al Kα X-ray source, hemispherical analyzer, multichannel detector, and low-energy electron flood gun for charge neutralization. For elemental composition determination spectra were acquired at an analyzer pass energy of 150 eV. The high-resolution C 1s spectra were acquired at an analyzer pass energy of 50 eV. The photoelectron takeoff angle (the angle between the sample normal and the input axis of the energy analyzer) for all XPS experiments was 55°. This takeoff angle corresponds to a sampling depth of approximately 5 nm. One or two spots on one or two replicates were analyzed for each sample treatment. The Service Physics ESCAVB Graphics Viewer program was used to determine peak areas, calculate the elemental compositions from those peak areas, and peak-fit the high-resolution spectra. The binding energy scale was calibrated by assigning the hydrocarbon peak in the C 1s high-resolution spectra to a binding energy of 285.0 eV. Further details of the XPS analysis procedures are described in ref 13.

2.2.2. Toluidine Blue: A Colorimetric Method. The toluidine blue (TB) colorimetric method previously described by Kato and Ikada[20] has been adapted for the PET samples used in our studies.[13] The protocol used was the following: 50 mL of a 5×10^{-4} M TB aqueous solution was prepared, and 0.2 mL of a 2-amino 2-methyl propanol buffer solution was added to reach and maintain the solution pH at 10. The sample was placed in 6 mL of the TB solution at 30 °C for 6 h. Noncomplexed TB molecules were removed by rapid washing of the sample with a basic aqueous solution (NaOH, 5×10^{-4} M, pH 9) for 30 min. Then, each sample was placed in 5−15 mL of an aqueous acetic acid solution (50%, v/v) for 24 h to obtain complete decomplexation of TB from the sample. TB assays were done on both ozonated and ozonated/grafted surfaces. To quantify the amount of NaSS grafted to a given ozonated PET surface the amount of TB complexed to the ozonated surface was subtracted from the amount of TB complexed to the corresponding ozonated/grafted surface.

The decomplexation solution was analyzed by UV−vis spectroscopy. TB has an absorption peak at 633 nm with an extinction coefficient of 50 000 L/(mol cm). It was assumed that a 1:1 complex between one TB molecule and one SO_3^- group is formed on the grafted surfaces. Therefore, the grafting ratio (GR) was calculated as follows

$$\text{GR (mol of grafted polymer/g fabric)} = CV/m$$

where C is the molar concentration of TB (in mol/L), V is the acetic acid volume (in L), and m is the mass of fabric (in g).

2.3. Biological Characterization. *2.3.1. Serum Albumin Adsorption Measurements.* Prior to human serum albumin (HSA) adsorption the PET fabrics were rinsed and equilibrated in PBS. Then the PBS was removed, and each fabric sample was covered with 1 mL of radiolabeled HSA ([^{125}I] HSA, 5 μCi/mL, CIS-BIO) in PBS. The adsorption onto the grafted and nongrafted PET fabrics was done from stirred HSA/PBS solutions at various concentrations for 45 min at room temperature. After the 45 min of adsorption each fabric sample was rinsed three times with 2 mL of PBS, aspirated, and then removed and counted in a gamma counter (Willco Wizard 1470). Each measurement was performed in triplicate.

2.3.2. McCoy Fibroblast Cell Culture. The human McCoy fibroblast cell line was purchased from the American Type Cultures Collection (No. CRL-1696) and stored frozen. Cells were cultured in 25 cm^2 tissue culture flasks with DMEM (Invitrogen) supplemented with 10% fetal calf serum (10% FCS−DMEM) and 1% antibiotics (penicillin−streptomycin, Invitrogen) at 37 °C under a humidified atmosphere in a CO_2 (5%) incubator (ASSAB T304 GF). The media was changed every 3 days. Cells between passage 10 and 15 were used for experiments in this study.

2.3.3. Kinetics of Cell Adhesion. Kinetics of cell adhesion was performed as follows: 10^6 cells were seeded onto grafted and nongrafted PET fabric samples and incubated for 0.5, 1, 4, and 24 h. Then the adhered cells were quantified by measurement of extracted total proteins.[21] The protein assay was performed by a colorimetric method[22] (BCA, Interchim). Cell adhesion percentages were expressed as the percentage of the number of cells adhered relative to the number of cells seeded.

2.3.4. Adhesion Strength. Adhesion strength of cells seeded on grafted and nongrafted PET fabrics was evaluated after preincubation of surfaces with 10% FCS−DMEM or normal human plasma (NHP).

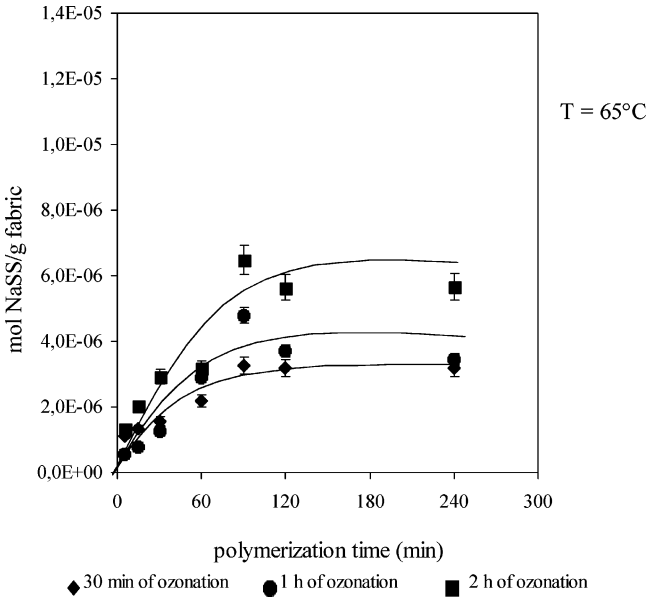

Figure 1. Grafting ratios of pNaSS on PET fabric ozonated for 30, 60, or 120 min: Toluidine blue colorimetry measurements. The grafting reaction was carried out at 65 °C for times up to 240 min.

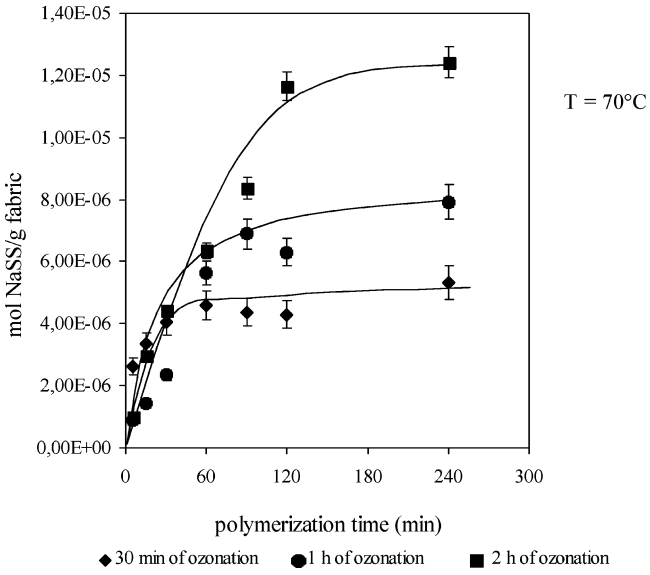

Figure 2. Grafting ratios of pNaSS on PET fabric ozonated for 30, 60, or 120 min: Toluidine blue colorimetry measurements. The grafting reaction was carried out at 70 °C for times up to 240 min.

The 1×1.3 cm^2 PET fabric samples were first incubated with 1 mL of 10% FCS−DMEM or NHP at 37 °C for 1 h while stirring, then washed twice with 1 mL of PBS. Fibroblasts, 2×10^6 cell/mL in DMEM, were incubated at 37 °C on the PET fabric samples for 1 h. Nonadhering cells were removed by rinsing the PET fabrics with PBS. Then the rinsed PET fabrics were placed on a rotating plate, and a centrifugal force (0−110 rpm) was applied for 10 min to the adhering cells on the fabrics. The cells detached by application of the centrifugal force were collected and counted. The cells remaining on the PET fabrics after application of the centrifugal force were then detached using a lysis buffer (0.5% Triton (Acros Organics), 150 mM NaCl, 150 mM PMSF (Sigma), 0.02% sodium azide (Fluka), and 2 mM EDTA in PBS) and counted. The following two types of cell counting methods were used for quantifying the number of cells in each solution: measurement of total cell proteins by the BCA assay and total cell DNA by Hoescht technique 33258 (Sigma). The centrifugal applied force can be translated into a mechanical force,[23,24] stress shear (τ). For each experiment τ_{50} was determined as the shear stress corresponding to the strength where 50% of the cells are detached.

2.3.5. Cell Morphology and Distribution. Fibroblast cells (50 000 cells/well) were seeded onto grafted and nongrafted PET fabric samples previously incubated with 10% FCS−DMEM then allowed to grow for either 4 or 6 days. Proliferating cells were then incubated away from light with fluorescent dyes for 30 min at room temperature: (a) 5 μM calcein AM solution (Interchim) or (b) 5 μg/mL acridine orange solution (Invitrogen). The morphologies of the proliferating cells were observed with a fluorescence microscope (Axiolab, Zeiss, Germany) that had an attached digital camera (Diagnostic Instruments, USA).

3. Results

3.1. pNaSS Grafting onto the PET Samples. *3.1.1. Toluidine Blue Characterization.* Figure 1 presents pNaSS grafting kinetics at $T = 65$ °C, as measured by TB colorimetry. Regardless of the ozonation time, the GR reaches a maximum after 90 min of polymerization. The influence of ozonation time can be seen by following the increase of GR maximum values from 3.5×10^{-6} to 5.5×10^{-6} mol/g fabric as the ozonation time increases from 30 to 120 min.

Grafting kinetics obtained at $T = 70$ °C are shown in Figure 2. There is a strong influence of temperature on the GR, which can double by increasing the temperature by 5 °C. For example, samples ozonated for 2 h reach a GR of 1.2×10^{-5} mol pNaSS/g fabric when reacted at 70 °C. However, it is also possible that too long ozonation times can degrade or alter the PET fabric properties. For this reason the optimal time of ozonation was chosen to be 30 min. After 30 min of ozonation no weight loss of the samples could be detected. Also, scanning electron microscopy did not detect any increase in surface roughness after this treatment. At 70 °C, after 30 min of ozonation, the maximum GR value of 4.5×10^{-6} is reached after 1 h of polymerization. These conditions were used to prepare samples for the biological tests.

3.1.2. XPS Characterization. The results from the XPS-determined elemental compositions of the PET fabric samples are summarized in Table 1. The theoretical XPS values expected for PET and pNaSS, based on their stoichiometry, are also included in Table 1 for comparison. The untreated PET surface showed slightly more carbon than expected theoretically. This is typical for PET and is probably due to the adsorption of a small amount of an adventitious hydrocarbon layer onto the PET surface. Ozone treatment of the surface did not significantly change the surface composition of the PET samples. This is consistent with previous XPS results that showed no significant difference between the untreated PET film surfaces and those ozonated for 30 or 60 min.[13] The reason that no significant differences were detected by XPS for the PET fabric samples was likely that (1) the ozone treatment conditions were rather mild and (2) the species produced by ozonation are reactive. Because it was several days after the ozonation treatment before the XPS measurements were done, the ozonated surfaces had probably already converted back to a state similar to untreated PET. Previous contact angle measurements on PET films showed changes in surface energetics of the ozonated PET films with the polar component of the surface energy increasing with ozonation time.[13] The roughness and woven fiber nature of the PET fabric samples prevented contact angle measurements of the PET fabric samples.

After ozonation and pNaSS grafting the carbon and oxygen concentrations decreased while the sulfur and sodium concentrations increased, as expected based on the theoretical compositions of PET and pNaSS. Unlike the PET film samples, significant addition of pNaSS was observed at all grafting times

Table 1. XPS-Determined Elemental Compositions of Untreated, Ozonated, and Ozonated Plus pNaSS-Grafted PET Fabric Samples[a]

	XPS atomic percent					
sample type	carbon	oxygen	sodium	sulfur	silicon	other
PET (theory)	71.4	28.6				
untreated PET	75 ± 1.3.3	24.7 ± 1.3				
30 min ozone	76.0 ± 2.4	23.8 ± 2.5				trace N
30 min ozone plus 30 min NaSS grafting	68.7 ± 1.6	21.6 ± 2.3	4.2 ± 0.4	5.0 ± 0.6	trace	trace N
30 min ozone plus 60 min NaSS grafting	68.3 ± 0.5	22.9 ± 0.7	4.0 ± 0.1	4.2 ± 0.5	0.6 ± 0.3	
30 min ozone plus 180 min NaSS grafting	66.6 ± 2.8	22.3 ± 2.4	5.1 ± 1.8	5.6±0.6	trace	trace P
NaSS (theory)	61.5	23.1	7.7	7.7		

[a] The XPS elemental compositions expected based on the stoichiometry of PET and pNaSS are also included in the table for comparison. Values are reported as averages ± one standard deviation. Trace means approximately 1 at. % or less of the element was detected in one replicate.

Table 2. XPS High-Resolution C 1s Results for Untreated, Ozonated, and Ozonated Plus NaSS-Grafted PET Fabric Samples[a]

	XPS C 1s percent			
sample type	C−C/C−H	C−O/C−SO_3	O−C═O	shakeup satellite
PET (theory)	60	20	20	
untreated PET	56 ± 4	25 ± 3	17 ± 1	3 ± 1
30 min ozone	61 ± 5	22 ± 4	16 ± 1	2 ± 1
30 min ozone plus 30 min pNaSS grafting	75 ± 5	17 ± 5	6 ± 2	2 ± 1
30 min ozone plus 60 min pNaSS grafting	82 ± 1	11 ± 2	5 ± 1	2 ± 1
30 min ozone plus 180 min pNaSS grafting	83 ± 5	11 ± 6	4 ± 1	1 ± 1
pNaSS (theory)	87.5	12.5		

[a] The XPS carbon species expected based on the stoichiometry of PET and NaSS are also included in the table for comparison. Values are reported as averages ± one standard deviation.

(30, 60, and 180 min). Similar XPS elemental compositions for all three grafting times are consistent with the similar GRs measured by TB colorimetry for 30 min ozonated samples grafted at 70 °C for 30−120 min (Figure 2). The grafting of pNaSS onto the PET surface should result in equal amounts of sodium and sulfur detected by XPS. Within the experimental error, this was true for all three pNaSS-grafted samples. Note that the XPS standard deviations increased significantly for the 180 min grafted sample. Variations in composition both from spot-to-spot on a replicate and from replicate-to-replicate were responsible for the increase in standard deviations. There was also a small amount of silicon detected (corresponding to significantly less than a monolayer of poly(dimethyl siloxane) (PDMS)) on the pNaSS-grafted surfaces. The presence of silicone is probably due to the introduction of small amounts of PDMS contamination onto the PET surface during the grafting process from nearby sources. The XPS composition of pure PDMS is 25 at. % Si, 25 at. % O, and 50 at. % C.

The results from the analysis of the XPS high-resolution C 1s spectra are summarized in Table 2. Also included in Table 2 are the expected amounts of each carbon species, based on the stoichiometry of PET and pNaSS. The results in Table 2 are consistent with the XPS compositional results discussed in the previous paragraphs. No significant differences are observed between the untreated PET film surface and the PET films ozonated for 30 or 60 min. The amount of the C−C/C−H species detected at 285 eV in the untreated and ozonated films is slightly higher than expected from the stoichiometry of PET. After 30 min of ozonation followed by 180 min of pNaSS grafting a significant increase in the amount of C−C/C−H species along with significant decreases in the amounts of C−O and O−C═O species were detected, as shown in Figure 3. This is expected due to the increased amount of C−C/C−H species in pNaSS relative to PET.

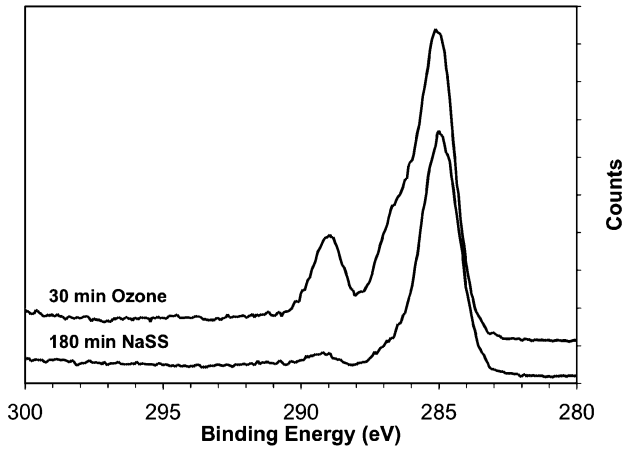

Figure 3. Representative XPS high-resolution C 1s spectra acquired from 30 min ozone-treated and 30 min ozone-treated plus 180 min NaSS-grafted PET fabrics. The introduction of the NaSS groups from the grafting process results in an increase in the C−C/C−H species at 285 eV and a decrease in the C−O and O−C═O species at 287 and 289 eV, respectively.

3.2. Biological Characterization of the PET Fabrics. *3.2.1. Serum Albumin Adsorption Measurements.* The adsorption of HSA onto pNaSS-grafted or nongrafted PET fabrics samples was performed to measure the protein adsorption capacities of both samples. HSA is a good reference protein for the measurement of the protein accessible surface area because it

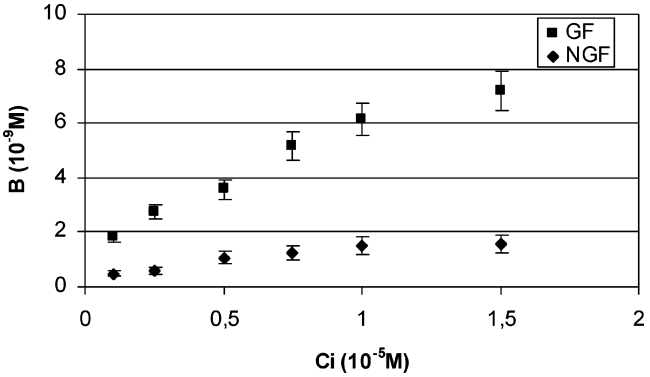

Figure 4. Typical isotherms of albumin adsorption onto pNaSS-grafted (■ GF) and nongrafted (◆ NGF) PET fabrics. HSA was ^{125}I radiolabeled. $n = 3$.

Table 3. Adsorption Parameters of [^{125}I] HSA onto pNaSS-Grafted and Nongrafted PET Fabrics[a]

PET sample	K_a (10^5 M^{-1})	B_{max} (10^{-9} mol HSA /sample)	ASA (cm^2/g)
nongrafted	2.7	7.2	861
pNaSS-grafted	3.7	1.6	3900

[a] ASA = accessible surface area to HSA protein, B_{max} = maximal adsorption capacity, K_a = affinity constant.

adsorbs onto the majority of polymeric surfaces in an almost identical and nonspecific manner.[25,26]

HSA isotherms (see Figure 4 for examples of typical isotherms) were used to prepare Scatchard plots. From the Scatchard plots the affinity constant (K_a) and the amount of adsorbed protein at saturation (B_{max}) were calculated. Table 3 lists the K_a and B_{max} values expressed in M^{-1} and μg HSA/mg fabric, respectively. Results show that the affinity constant K_a is about $\sim 3 \times 10^5$ M^{-1} for both grafted and nongrafted fabric samples. In contrast, the B_{max} values are very different for the two types of samples. B_{max} was 4 times higher on the grafted fabrics compared to the nongrafted fabrics. The observed affinity constant values of the two materials are consistent with the values previously reported for albumin adsorption onto polymeric surfaces.[27] The significant increase in the capacity of the pNaSS-grafted PET surface to adsorb protein is not surprising because the grafting of a polyanionic, water-soluble polymer makes the surface more hydrophilic and more swellable in PBS compared to nongrafted PET.

To scale the data for comparison in the remaining biological characterization experiments, the surfaces were normalized by their measured area available for protein adsorption. To do this the B_{max} values were converted from μg HSA/mg fabric to μg of HSA adsorbed per cm^2 of available surface area as described by Sebastien et al.[28] This method assumes that 0.12 μg of HSA adsorbs per cm^2 of available surface.

3.2.2. Kinetics of Fibroblast Adhesion on PET Fabrics. A kinetic analysis of cell adhesion in 10% FCS−DMEM was done for grafted and nongrafted PET fabrics to determine the optimal required time for McCoy fibroblasts to adhere to the surfaces. Approximately 10^6 cells/fabric were seeded onto the samples and then incubated for varying times (0.5, 1, 4, and 24 h). The number of adhered cells was quantified by using a total protein assay. Figure 5 shows the number of adhering cells, expressed as a percentage of the number of seeded cells, as a function of the incubation time. The results show that cell adhesion is very rapid on these surfaces, reaching levels of 90% after 1 h of incubation. Thus, a 1 h incubation time was selected for the cell adhesion strength experiments.

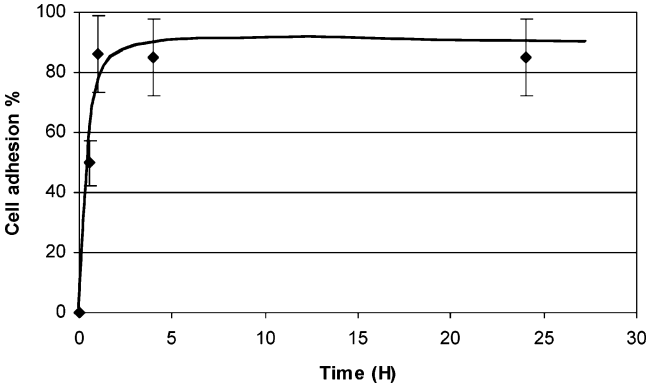

Figure 5. Kinetics of McCoy fibroblast adhesion onto pNaSS-grafted PET fabrics. Cell culture conditions: 10% FCS supplemented medium. ($n = 6$).

3.2.3. Measurement of Fibroblast Adhesion Strength on PET Fabrics. The study of the adhesion strength on PET fabrics was carried out in a medium with different protein concentrations to evaluate the role of the adsorbed proteins on the cell adhesion process. Prior to the adhesion strength measurements the PET fabrics were coated with proteins from either 10% FCS−DMEM or NHP. After seeding, incubating, and rinsing, the cell adhesion strength for both pNaSS-grafted and nongrafted PET fabrics was determined by applying variable centrifuge forces to fabrics with adhered cells. The angular speed initially expressed in rpm was translated into a mechanical strength τ in dyn/cm^2.[23,24] The strength varies linearly with the radial position of cells (r) according to the equation

$$\tau = 0.8r\sqrt{\rho\mu\omega^3}\ (\text{dyn/cm}^2)$$

where r is the radial distance from the center (25 cm), ρ is the fluid density (near 1 g/cm^3 [23]), μ is the fluid viscosity (0.85 cP[23]), and ω is the angular velocity.

For each experiment the shear stress corresponding to the strength where 50% of cells are detached, τ_{50}, was determined to compare the adhesion strengths of cells on pNaSS-grafted and nongrafted PET fabrics.

3.2.3.1. Cell Adhesion Strengths with Supplemented Medium: 10% FCS−DMEM. The 10% FCS−DMEM, a supplemented medium, was chosen because it is the reference medium for cell culture. This medium contains (1) proteins from serum but at concentrations 10 times lower than that of NHP[29] and (2) does not contain fibrinogen (3 g/L) and some coagulation factors. The application of shear stress from 0 to 33 dyn/cm^2 to cells adhering on both grafted and nongrafted PET fabrics, previously incubated with 10% FCS−DMEM, led to strong differences in the percentages of adhering cells (Figure 6). These results demonstrate that different adhesion strengths are obtained for cells grown on grafted versus nongrafted PET fabrics.

The majority of cells are rapidly detached from the nongrafted PET surfaces at low shear stresses: 50% detached by 1 dyn/cm^2, 70% by 4 dyn/cm^2, and 90% by 13 dyn/cm^2 (Figure 6). In contrast, on the pNaSS-grafted PET surfaces it was necessary to apply shear stresses of 13 dyn/cm^2 to detach 50% of cells and 18 dyn/cm^2 to detach 70% of the cells. The τ_{50} values for the two surfaces—which give the stress necessary to detach 50% of the adhered cells and therefore reflect the adhesion strength of cells—are compared in Table 4. These results suggest that the strength of cell adhesion is about 12 times higher on pNaSS-grafted PET compared to nongrafted PET ($p < 0.05$, analysis of variation). These differences show that the cell/protein/surface interactions, in the absence of adsorbed fibrinogen, are weaker

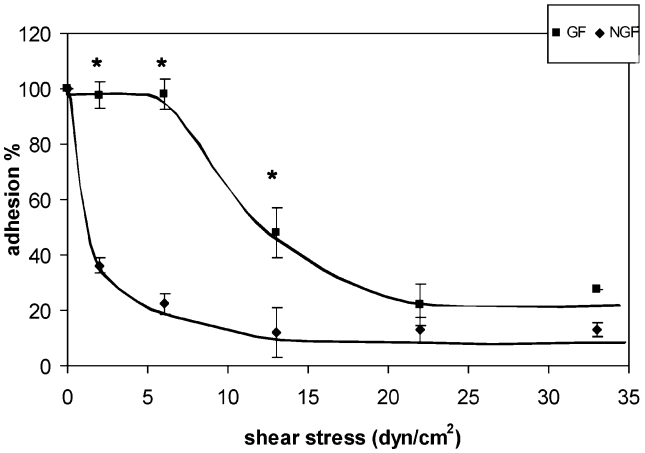

Figure 6. Variation of the cell adhering percentage vs the applied shear stress τ (dyn/cm^2) for pNaSS-grafted (■ GF) and nongrafted (◆ NGF) PET fabrics previously adsorbed with 10% FCS supplemented medium. ($n = 6$, * $p < 0.05$).

Table 4. Experimental τ_{50} Values for Nongrafted and pNaSS-Grafted PET Fabrics under Different Protein Conditions[a]

PET sample	τ_{50} (dyn/cm^2) 10% FCS− DMEM	τ_{50} (dyn/cm^2) NHP
nongrafted	1	4
pNaSS-grafted	12	>33

[a] τ_{50} represents the required shear stress to detach 50% of the adhering cells.

on the nongrafted PET compared to those on the pNaSS-grafted PET. This suggests that the adsorbed proteins on the pNaSS-grafted PET surface are able to more effectively attach cells.

3.2.3.2. Cell Adhesion Strengths with Supplemented Medium: NHP. When PET fabric samples were preincubated with platelet poor NHP, the cell seeding and adhesion strength measurements were carried out in culture medium that did not contain proteins. Comparison to the results described above for protein coating from 10% FCS−DMEM, NHP allows evaluation of the influence of protein concentration (10×) and the presence of fibrinogen on cell adhesion strength. Fibrinogen contains RGD sequences that can play a role in the cell adhesion process.[30]

The percentages of adhering cells plotted versus shear stress are presented in Figure 7. Significant differences are observed between the pNaSS-grafted and nongrafted PET fabric samples, showing that the cell adhesion process depends on the chemistry of the surface and its adsorbed protein layer. It is significant to note that for the pNaSS-grafted surfaces coated with proteins from NHP the percentage of adhering cells is constant (∼80−90%) at all applied shear stresses measured (1−33 dyn/cm^2). So the τ_{50} value of the pNaSS-grafted PET fabric cannot be measured precisely from the range of applied centrifugal forces in this study and is listed in Table 4 as >33 dyn/cm^2 (the highest applied sheer stress in this study). In contrast significant detachment of cells from the nongrafted PET fabric was observed even at low shear stress (<10 dyn/cm^2). The τ_{50} for the nongrafted PET fabric is approximately 4 dyn/cm^2. Coating the surfaces with NHP, compared to 10% FCS−DMEM, increased the cell adhesion for both the nongrafted (1−4 dyn/cm^2) and pNaSS-grafted (12 to >33 dyn/cm^2) PET surfaces, showing that the different protein compositions in these media do affect cell adhesion. In particular, the presence of fibrinogen and its known role in cell adhesion are consistent with the higher τ_{50} values observed from the NHP-coated fabric samples and

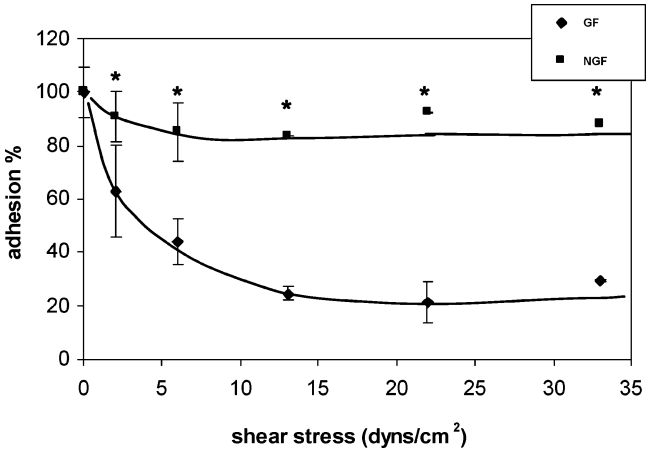

Figure 7. Variation of the cell adhering percentage vs the applied shear stress τ (dyn/cm^2) for pNaSS-grafted (■ GF) and nongrafted (◆ NGF) PET fabrics previously adsorbed with NHP. ($n = 6$, * $p < 0.05$).

show the strong role of adsorbed plasma proteins in cell/protein/surface interactions. For both coating solutions the cell adhesion strengths were more than 10 times higher on the pNaSS-grafted surfaces compared to those on the nongrafted surfaces.

3.2.4. Cell Morphology and Distribution. The observation of cell morphology and distribution at days 4 and 6 (Figure 8) highlighted the following important information about cell/surface interactions:

(1) Cells are living when adhering and proliferating onto grafted and nongrafted PET surfaces, as shown by the green color of the cells. After calcein AM enters the cell it is converted to calcein by esterase cleavage and then emits green fluorescence. Acridine orange also emits green fluorescence when bound to the double-stranded DNA of living cells. These fluorescence results show that the PET surfaces are not cytoxic.

(2) In the case of the nongrafted PET surfaces, cells had a round shape even after 4 and 6 days of proliferation, showing that cells were able to proliferate but not to spread (Figure 8A). In addition, cells proliferated as clusters with a heterogeneous distribution, as illustrated in Figure 8C.

(3) In the case of pNaSS-grafted PET, cells were well spread at days 4 and 6 and homogeneously distributed all along the fibers.

4. Discussion

Both XPS and TB colorimetry showed that pNaSS was successfully grafted onto the surface of PET fabrics. In comparison to previous experiments on PET films,[13] both the amount and the kinetics of pNaSS grafting differed between the two types of PET samples. In the PET film study,[13] the grafting ratio was expressed in grams of grafted polymer versus surface area of film in cm^2. For the current PET fabric study the grafting was expressed per gram of fabric because the specific surface area of the fabric samples is unknown. Nevertheless, XPS results show that significantly more pNaSS was grafted onto the PET fabrics compared to the PET films, especially at short reaction times. For example, after 30 min of ozonation and 30 or 60 min of reaction at 70 °C the XPS sulfur and sodium concentrations (which are directly related to the grafted pNaSS concentration) were an order of magnitude higher on the PET fabrics compared to those on the PET films. Even after 180 min of reaction at 70 °C the fabric samples still show 50% higher XPS sulfur and sodium concentrations than the film

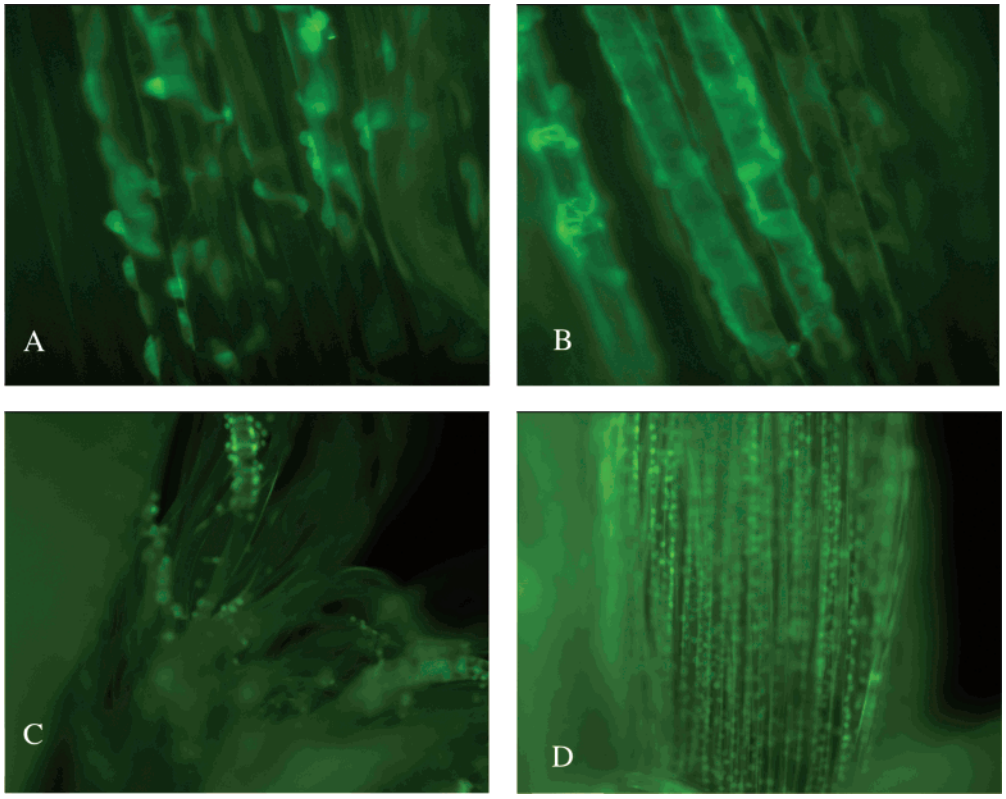

Figure 8. Morphology and distribution of adhering and proliferating cells onto PET fibers with calcein and acridine orange staining: nongrafted fibers (A, day 4; C, day 6), pNaSS-grafted (B, day 4; D day 6).

samples. However, the XPS elemental compositions and high-resolution spectra of the pNaSS-grafted PET fabrics activated with a 30 min ozone treatment never reached the values expected for 100% pNaSS. This means that under these experimental conditions the thickness of the pNaSS-grafted layer was less than the XPS sampling depth of approximately 5 nm. It is also possible that the pNaSS-grafted layer could be patchy, but the TB results show that the amount of NaSS grafted to the PET surfaces was higher than the amount needed to completely cover the surface of the PET fabrics. Also, the homogeneous distribution of cells on the grafted surface is not consistent with a patchy overlayer of pNaSS.

TB colorimetry results indicated that the grafting of pNaSS onto the PET films and fabrics proceeded at different rates. In the case of PET films only small amounts of grafting were detected during the first 60 min of reaction whereas significant increases in the amount of grafted pNaSS were observed between 60 and 120 min.[13] In contrast, a steady and significant increase of pNaSS grafting was observing during the first 60 min of reaction on the PET fabrics, then little, if any, further increase was observed beyond 60 min of reaction. This indicates that the pNaSS grafting process is more rapid on the PET fabric samples. This can be explained by the higher specific surface area of woven PET fabrics for which the 30 min ozone treatment is more effective at creating pNaSS reaction sites (e.g., surface radicals) compared to the smooth PET film surface.

Both the XPS and the TB results are consistent with the grafting of a thin (<5 nm in thickness) surface layer of pNaSS onto the PET fabrics. As the surface chemistry of pNaSS differs significantly from that of PET, the presence of this thin surface layer of grafted pNaSS is expected to have a pronounced effect on protein adsorption and cell adhesion. For example, Migonney and co-workers have previously shown that poly(methyl methacrylate) (PMMA) surfaces with sulfonate and carboxylic acid groups showed an enhanced affinity for fibronectin over albumin, resulting in adsorbed protein films that were significantly enriched in fibronection compared to the PMMA surface without anionic groups.[31−33] Moreover, the conformation of fibronectin was observed to vary with the surface concentrations of the sulfonate and carboxylic acid groups.[31−33] These differences in the concentration and conformation of adsorbed proteins can have a significant influence on cell interactions with synthetic biomaterials because protein adsorption is one of the first events that occurs when a biomaterial is placed in contact with biological fluids.[26] Then, cells such as macrophages and fibroblasts will migrate to the biomaterial surface and interact with the adsorbed protein film. It is well-documented that the adhesion of fibroblasts is mediated by adhesion proteins such as fibronectin,[34,35] vitronectin, collagen,[36] and fibrin.[37] Among these proteins, fibronectin and vitronectin are two ubiquitous glycoproteins that are synthesized by a large variety of cell types. These two proteins have been proposed to play a major role in the cell adhesion process on biomaterials, even when present at low concentrations in plasma.[31−33] Both proteins were present in the 10% FCS−DMEM and NHP solutions used to precoat the PET surfaces prior to the cell adhesion experiments.

The factor of 4 increase in HSA adsorption on pNaSS-grafted PET fabrics compared to that on nongrafted PET fabrics is consistent with the results published by Kishida et al.[38] that showed that the capacity of polymer surfaces to adsorb albumin depends on their surface energy and hydrophobic/hydrophilic nature. In addition others have shown that as the surfaces of PET films become more hydrophilic the amount of adsorbed protein increases.[39,40]

As the protein film on a material provides the anchoring points for cell attachment, the different amounts of protein adsorption and different cell adhesion strengths observed on the pNaSS-grafted PET fabrics compared to those on the nongrafted PET fabrics indicate that the protein films formed on the two PET fabric surfaces are different. The order of magnitude

increase in cell adhesion observed upon pNaSS grafting indicates that the protein films on the pNaSS-grafted PET fabrics contain more adhesive proteins such as fibronectin and vitronectin than the protein films on nongrafted PET fabrics. This is consistent with previous studies that have shown that polymer surfaces with anionic groups show an enrichment of adsorbed fibronectin.[31,33] Also, the same studies showed that the fibronectin conformation depended on the chemical composition of the surface anionic groups. Differences in both the amount of adhesive proteins and their confirmation can both affect the surface concentration of cell binding domains (e.g., RGD motifs) on pNaSS-grafted PET surfaces. This will in turn affect cell attachment and adhesion. The fact that pNaSS-grafted PET fabrics bind fibroblasts significantly more strongly than nongrafted PET fabrics indicates that the adsorbed protein films on the pNaSS-grafted surface contain more adsorbed adhesive proteins in conformations more favorable for cell adhesion.

It is also interesting to note that the strength of cell adhesion increases further when the pNaSS-grafted PET fabrics are precoated with NHP instead of 10% FCS−DMEM. Stanislawski et al.[41] identified the major proteins adsorbed from NHP onto materials currently used in the fabrication of synthetic ligaments. They showed that the percentages of adsorbed proteins onto PET fibers were albumin 48%, Apo I 39%, fibrinogen 8%, and Apo E 5%, with other plasma proteins present at lower levels. Because fibrinogen is not present in 10% FCS−DMEM, the higher fibroblast adhesion observed from pNaSS-grafted PET fabrics precoated with NHP is likely due to the presence of adsorbed fibrinogen in the protein films deposited from NHP. In the samples precoated with NHP, fibrinogen could increase the strength of fibroblast adhesion by interacting directly with the fibroblasts or through a competitive protein adsorption process that produces a higher surface concentration of adhesive proteins in favorable conformations for cell attachment. The fact that with NHP precoating the differences in cell adhesion strengths between pNaSS-grafted PET fabrics and nongrafted PET fabrics is even larger than for the same samples coated with 10% FCS−DMEM is consistent with other studies that have shown that the adsorption of fibrinogen is higher on sulfonated polyurethane surfaces as compared to that on nonfunctionalized polyurethane surfaces.[42,43]

It is worthy to note that the observed differences in the adhesion strengths of cells onto pNaSS-grafted PET and nongrafted PET fabrics were well correlated to the differences in the morphology and distribution of adhering cells. Cells were totally spread and homogenously distributed on grafted surfaces whereas they were still round shaped, not spread, and distributed as clusters on the nongrafted PET surfaces.

5. Conclusions

This study showed that pNaSS could be successfully grafted onto the surface of PET fabrics and that the pNaSS-grafted PET fabrics exhibited improved biological responses in terms of increased protein adsorption capacities and increased strength of cell adhesion. The amount of pNaSS grafted onto the PET fabrics depended on the length of the ozone activation treatment, the grafting temperature, and the grafting time. Increasing the ozonation time from 30 to 120 min resulted in an increase in the amount of pNaSS that could be grafted. Increasing the grafting temperature from 65 to 70 °C also significantly increased the amount of pNaSS that could be grafted. An increase in the amount of grafted pNaSS with reaction time was observed during the first 60 min of grafting. From 60 to 240 min the amount of grafted pNaSS remained relatively constant. Thus, samples were prepared for the biological experiments using a 30 min ozone treatment and a 60 min polymerization reaction at 70 °C. The pNaSS-grafted PET fabrics adsorbed a factor of 4 more HSA than the nongrafted PET fabrics. The strength of fibroblast adhesion increased by a factor of at least 10 on the pNaSS-grafted PET fabrics compared to that on the nongrafted PET fabrics. Also, the type of protein medium used to precoat the PET fabrics affected the strength of fibroblast adhesion. A small increase was observed for the nongrafted PET fabrics coated with NHP compared to 10% FCS−DMEM. In contrast, greater than a factor of 3 increase in the strength of fibroblast adhesion was observed when the pNaSS-grafted PET fabrics were coated with NHP instead of 10% FCS−DMEM. These results indicate that the composition of the protein film on the pNaSS-grafted compared to that on the nongrafted PET fabrics is different as are the protein film compositions deposited from 10% FCS−DMEM compared those from NHP.

Acknowledgment. The authors thank Bernard Brulez for his helpful contribution and the Lars Society (Arc sur Tille, France) for partial financial support of this work. The XPS experiments were done at NESAC/BIO, which is supported by a grant from the National Institute of Biomedical Imaging and Bioengineering (Grant No. EB-002027).

References and Notes

(1) Desgranges, P.; Caruelle, J. P.; Carpentier, G.; Barritault, D.; Tardieu, M. Beneficial use of fibroblast growth factor 2 and RGTA, a new family of heparan mimics, for endothelialization of PET prostheses. *J. Biomed. Mater. Res.* **2001**, *58* (1), 1−9.

(2) Moroni, L.; Licht, R.; de Boer, J.; de Wijn, J. R.; van Blitterswijk, C. A. Fiber diameter and texture of electrospun PEOT/PBT scaffolds influence human mesenchymal stem cell proliferation and morphology, and the release of incorporated compounds. *Biomaterials* **2006**, *27* (28), 4911−4922.

(3) Park, S.; Bearinger, J. P.; Lautenschlager, E. P.; Castner, D. G.; Healy, K. E. Surface modification of poly(ethylene terephthalate) angioplasty balloons with a hydrophilic poly(acrylamide-*co*-ethylene glycol) interpenetrating polymer network coating. *J. Biomed. Mater. Res.* **2000**, *53* (5), 568−576.

(4) Ramires, P. A.; Mirenghi, L.; Romano, A. R.; Palumbo, F.; Nicolardi, G. Plasma-treated PET surfaces improve the biocompatibility of human endothelial cells. *J. Biomed. Mater. Res.* **2000**, *51* (3), 535−539.

(5) Eberhart, A.; Zhang, Z.; Guidoin, R.; Laroche, G.; Guay, L.; De La Faye, D.; Batt, M.; King, M. W. A new generation of polyurethane vascular prostheses: Rara avis or ignis fatuus? *J. Biomed. Mater. Res.* **1999**, *48* (4), 546−558.

(6) Puskas, J. E.; Chen, Y. Biomedical application of commercial polymers and novel polyisobutylene-based thermoplastic elastomers for soft tissue replacement. *Biomacromolecules* **2004**, *5* (4), 1141−1154.

(7) Blanchemain, N.; Haulon, S.; Martel, B.; Traisnel, M.; Morcellet, M.; Hildebrand, H. F. Vascular PET prostheses surface modification with cyclodextrin coating: Development of a new drug delivery system. *Eur. J. Vasc. Endovasc. Surg.* **2005**, *29* (6), 628−632.

(8) Ueberrueck, T.; Tautenhahn, J.; Meyer, L.; Kaufmann, O.; Lippert, H.; Gastinger, I.; Wahlers, T. Comparison of the ovine and porcine animal models for biocompatibility testing of vascular prostheses. *J. Surg. Res.* **2005**, *124* (2), 305−311.

(9) McPherson, G. K.; Mendenhall, H. V.; Gibbons, D. F.; Plenk, H.; Rottmann, W.; Sanford, J. B.; Kennedy, J. C.; Roth, J. H. Experimental mechanical and histologic evaluation of the Kennedy ligament augmentation device. *Clin. Orthop. Relat. Res.* **1985**, (196), 186−195.

(10) Poddevin, N.; King, M. W.; Guidoin, R. G. Failure mechanisms of anterior cruciate ligament prostheses: In vitro wear study. *J. Biomed. Mater. Res.* **1997**, *38* (4), 370−381.

(11) Devita, P.; Hortobagyi, T.; Barrier, J.; Torry, M.; Glover, K. L.; Speroni, D. L.; Money, J.; Mahar, M. T. Gait adaptations before and after anterior cruciate ligament reconstruction surgery. *Med. Sci. Sports Exercise* **1997**, *29* (7), 853.

(12) Dominkus, M.; Sabeti, M.; Toma, C.; Abdolvahab, F.; Trieb, K.; Kotz, R. I. Reconstructing the extensor apparatus with a new polyester ligament. *Clin. Orthop. Relat. Res.* **2006**, *453*, 328−334.
(13) Ciobanu, M.; Siove, A.; Gueguen, V.; Gamble, L. J.; Castner, D. G.; Migonney, V. Radical graft polymerization of styrene sulfonate on poly(ethylene terephthalate) films for ACL applications: "Grafting from" and chemical characterization. *Biomacromolecules* **2006**, *7* (3), 755−760.
(14) Brunet, P.; Charrois, O.; Degeorges, R.; Boisrenoult, P.; Beaufils, P. Reconstruction of acute posterior cruciate ligament tears using a synthetic ligament. *Rev. Chir. Orthop. Reparatrice Appar. Mot.* **2005**, *91* (1), 34−43.
(15) Nau, T.; Lavoie, P.; Duval, N. A new generation of artificial ligaments in reconstruction of the anterior cruciate ligament. Two-year follow-up of a randomised trial. *J. Bone Jt. Surg., Br. Vol.* **2002**, *84* (3), 356−360.
(16) Lavoie, P.; Fletcher, J.; Duval, N. Patient satisfaction needs as related to knee stability and objective findings after ACL reconstruction using the LARS artificial ligament. *Knee* **2000**, *7* (3), 157−163.
(17) Migonney, V.; Pavon-Djavid, G.; Siove, A.; Ciobanou, M.; Brulez, B. Ligament prothétique biomimétique et procédé d'obtention. PCT BF 0300497, 2003.
(18) Poddevin, N.; Cronier, B.; Marois, Y.; Delagoutte, J. P.; Mainard, D.; Jaeger, J. H.; Belanger, A. Y.; King, M. W.; Guidoin, R. Macroscopic, histologic and ultrastructural study of 89 prostheses of anterior cruciate ligament excised because of prosthesis failure. *Rev. Chir. Orthop. Reparatrice Appar. Motil.* **1995**, *81* (5), 410−418.
(19) Savarese, A.; Lunghi, E.; Budassi, P.; Agosti, A. Remarks on the complications following ACL reconstruction using synthetic ligaments. *Ital. J. Orthop. Traumatol.* **1993**, *19* (1), 79−86.
(20) Kato, K.; Ikada, Y. Selective adsorption of proteins to their ligands covalently immobilized onto microfibers. *Biotechnol. Bioeng.* **1995**, *47*, 557−566.
(21) Brooks, S. P.; Lampi, B. J.; Sarwar, G.; Botting, H. G. A comparison of methods for determining total body protein. *Anal. Biochem.* **1995**, *226* (1), 26−30.
(22) Smith, P. K.; Krohn, R. I.; Hermanson, G. T.; Mallia, A. K.; Gartner, F. H.; Provenzano, M. D.; Fujimoto, E. K.; Goeke, N. M.; Olson, B. J.; Klenk, D. C. Measurement of protein using bicinchoninic acid. *Anal. Biochem.* **1985**, *150* (1), 76−85.
(23) Garcia, A. J.; Ducheyne, P.; Boettiger, D. Quantification of cell adhesion using a spinning disc device and application to surface-reactive materials. *Biomaterials* **1997**, *18* (16), 1091−1098.
(24) Rezania, A.; Thomas, C. H.; Branger, A. B.; Waters, C. M.; Healy, K. E. The detachment strength and morphology of bone cells contacting materials modified with a peptide sequence found within bone sialoprotein. *J. Biomed. Mater. Res.* **1997**, *37* (1), 9−19.
(25) Andrade, J. D. Interfacial phenomena and biomaterials. *Med. Instrum.* **1973**, *7* (2), 110−119.
(26) Andrade, J. D.; Hlady, V. Plasma protein adsorption: The big twelve. *Ann. N. Y. Acad. Sci.* **1987**, *516*, 158−172.
(27) Brash, J. L.; Ten Hove, P. Protein adsorption studies on 'standard' polymeric materials. *J. Biomater. Sci., Polym. Ed.*. **1993**, *4* (6), 591−599.
(28) Sebastien, K.; Pavon-Djavid, G.; Migonney, V.; Kazatchkine, M.; Jozefowicz, M. C3b-like random copolymers: Biospecific interactions with complement receptor type one (CR1, CD35). *Int. J. Bio-Chromatogr.* **1997**, *3*, 313−328.
(29) Smith, P. K.; Krohn, R. I.; Hermanson, G. T.; Mallia, A. K.; Gartner, F. H.; Provenzano, M. D.; Fujimoto, E. K.; Goeke, N. M.; Olson, B. J.; Klenk, D. C. Measurement of protein using bicinchoninic acid. *Anal. Biochem.* **1985**, *150* (1), 76.
(30) Joshi, P.; Chung, C. Y.; Aukhil, I.; Erickson, H. P. Endothelial cells adhere to the RGD domain and the fibrinogen-like terminal knob of tenascin. *J. Cell Sci.* **1993**, *106* (1), 389−400.
(31) El Khadali, F.; Helary, G.; Pavon-Djavid, G.; Migonney, V. Modulating fibroblast cell proliferation with functionalized poly(methyl methacrylate) based copolymers: Chemical composition and monomer distribution effect. *Biomacromolecules* **2002**, *3* (1), 51−56.
(32) Evans, M.; Pavon-Djavid, G.; Hélary, G.; Legeais, J.-M.; Migonney, V. Vitronectin is significant in the adhesion of lens epithelial cells to PMMA polymers. *J. Biomed. Mater. Res.* **2004**, *69* (3), 469−476.
(33) Latz, C.; Pavon-Djavid, G.; Helary, G.; Evans, M.; Migonney, V. Alternative intracellular signaling mechanism involved in the inhibitory biological response of functionalized PMMA-based polymers. *Biomacromolecules* **2003**, *4* (3), 766−771.
(34) Hormann, H. Fibronectin—Mediator between cells and connective tissue. *Klin. Wochenschr.* **1982**, *60* (20), 1265−1277.
(35) Hormann, H. Fibronectin cell interaction. *Klin. Wochenschr.* **1986**, *64* (Suppl. 7), 51−53.
(36) Puschel, H.-U.; Chang, J.; Muller, P. K.; Brinckman, J. Attachment of intrinsically and extrinsically aged fibroblasts on collagen and fibronectin. *J. Photochem. Photobiol., B* **1995**, *27* (1), 39.
(37) Yang, W.; Wu, B.; Asakura, S.; Kohno, I.; Matsuda, M. Soluble fibrin augments spreading of fibroblasts by providing RGD sequences of fibrinogen in soluble fibrin. *Thromb. Res.* **2004**, *114* (4), 293.
(38) Kishida, A.; Iwata, H.; Tamada, Y.; Ikada, Y. Cell behaviour on polymer surfaces grafted with non-ionic and ionic monomers. *Biomaterials* **1991**, *12* (8), 786−792.
(39) Rouxhet, L.; Duhoux, F.; Borecky, O.; Legras, R.; Schneider, Y. J. Adsorption of albumin, collagen, and fibronectin on the surface of poly(hydroxybutyrate−hydroxyvalerate) (PHB/HV) and of poly(ϵ-caprolactone) (PCL) films modified by an alkaline hydrolysis and of poly(ethylene terephthalate) (PET) track-etched membranes. *J. Biomater. Sci., Polym. Ed.* **1998**, *9* (12), 1279−1304.
(40) Satriano, C.; Manso, M.; Gambino, G. L.; Rossi, F.; Marletta, G. Adsorption of a cell-adhesive oligopeptide on polymer surfaces irradiated by ion beams. *Biomed. Mater. Eng.* **2005**, *15* (1−2), 87−99.
(41) Stanislawski, L.; De Nechaud, B.; Christel, P. Plasma protein adsorption to artificial ligament fibers. *J. Biomed. Mater. Res.* **1995**, *29* (3), 315−323.
(42) Chen, Z.; Ward, R.; Tian, Y.; Malizia, F.; Gracias, D. H.; Shen, Y. R.; Somorjai, G. A. Interaction of fibrinogen with surfaces of end-group-modified polyurethanes: A surface-specific sum-frequency-generation vibrational spectroscopy study. *J. Biomed. Mater. Res.* **2002**, *62* (2), 254−264.
(43) Cornelius, R. M.; Brash, J. L. Effect of single-chain and two-chain high molecular weight kininogen on adsorption of fibrinogen from binary mixtures to glass and sulfonated polyurethane surfaces. *J. Biomed. Mater. Res.* **1997**, *37* (3), 314−323.

BM070344I